ACS Synthetic Biology
Cite This: ACS Synth. Biol. XXXX, XXX, XXX−XXX
Research Article
pubs.acs.org/synthbio

Development of a Genetically Encoded Biosensor for Detection of Polyketide Synthase Extender Units in *Escherichia coli*

Edward Kalkreuter,[†,‡,§] Aaron M. Keeler,[†,¶] Alexandra A. Malico,[†,¶] Kyle S. Bingham,[†,⊥] Anuran K. Gayen,[†] and Gavin J. Williams*[,†,‡]

[†]Department of Chemistry, North Carolina State University, Raleigh, North Carolina 27695, United States
[‡]Comparative Medicine Institute, North Carolina State University, Raleigh, North Carolina 27695, United States

Supporting Information

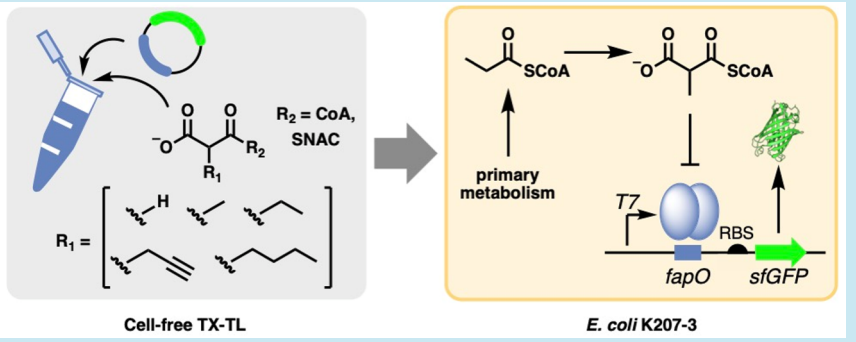

ABSTRACT: The scaffolds of polyketides are constructed via assembly of extender units based on malonyl-CoA and its derivatives that are substituted at the C2-position with diverse chemical functionality. Subsequently, a transcription-factor-based biosensor for malonyl-CoA has proven to be a powerful tool for detecting malonyl-CoA, facilitating the dynamic regulation of malonyl-CoA biosynthesis and guiding high-throughput engineering of malonyl-CoA-dependent processes. Yet, a biosensor for the detection of malonyl-CoA derivatives has yet to be reported, severely restricting the application of high-throughput synthetic biology approaches to engineering extender unit biosynthesis and limiting the ability to dynamically regulate the biosynthesis of polyketide products that are dependent on such α-carboxyacyl-CoAs. Herein, the FapR biosensor was re-engineered and optimized for a range of mCoA concentrations across a panel of *E. coli* strains. The effector specificity of FapR was probed by cell-free transcription−translation, revealing that a variety of non-native and non-natural acyl-thioesters are FapR effectors. This FapR promiscuity proved sufficient for the detection of the polyketide extender unit methylmalonyl-CoA in *E. coli*, providing the first reported genetically encoded biosensor for this important metabolite. As such, the previously unknown broad effector promiscuity of FapR provides a platform to develop new tools and approaches that can be leveraged to overcome limitations of pathways that construct diverse α-carboxyacyl-CoAs and those that are dependent on them, including biofuels, antibiotics, anticancer drugs, and other value-added products.

KEYWORDS: *malonyl-CoA, polyketide, biosensor, transcription factor, synthetic biology*

Engineered bacterial transcriptional regulators have contributed immensely to chemical and synthetic biology by providing highly modular and tunable devices for sensing small molecules.[1−3] By coupling them to fluorescent or chromogenic readouts, transcription-factor-based biosensors have been applied as tools that detect key metabolites, regulate biosynthetic circuits, guide metabolic engineering, and enable directed evolution of enzymes and pathways.[4−7] Yet, biosensors for the detection of natural products and their biosynthetic precursors are not yet widely available, limiting the ability of high-throughput strategies to be applied to many important classes of molecules. For instance, malonyl-CoA (mCoA, Figure 1) plays an integral role in cellular primary and secondary metabolism as a building block for fatty acids, phenylpropanoids, polyketides, and hybrid natural products.[8] Because of this, mCoA biosynthesis has been a longstanding target of metabolic engineering efforts.[9−13] Accordingly, genetically encoded biosensors for the detection of mCoA have been constructed using FapR, a transcriptional regulator found in nearly all Gram-positive bacteria that acts as a global regulator for fatty acid biosynthesis.[14] FapR has been characterized as the only member of its regulator family owing to its unique, highly dynamic structure.[15,16] Crystal structures of FapR indicate a dimer, whereby each monomer is comprised of a C-terminal ligand-binding domain and an N-terminal domain that binds to its cognate DNA operator, *fapO*. Dependent on the promoter, FapR has been shown to act as

Received: February 21, 2019

DOI: 10.1021/acssynbio.9b00078
ACS Synth. Biol. XXXX, XXX, XXX−XXX

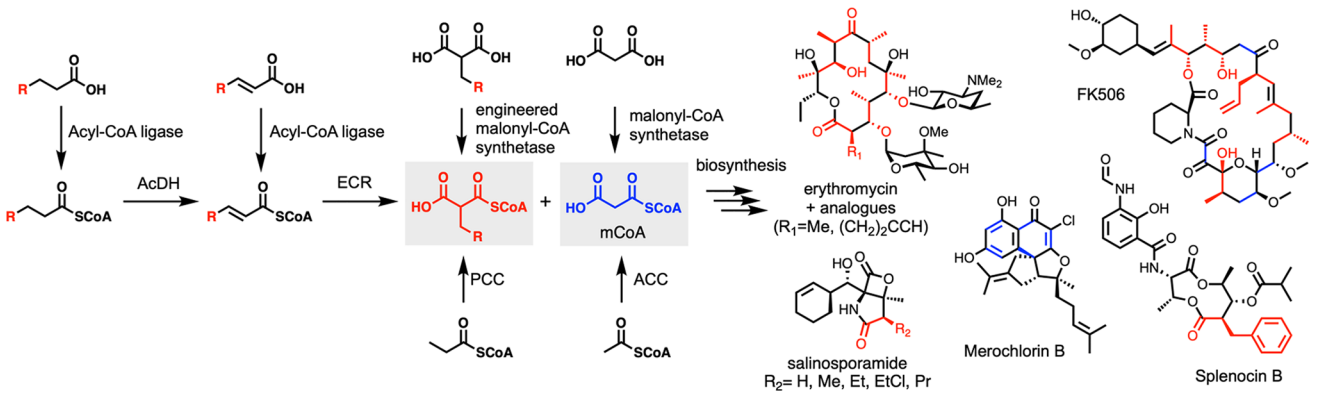

Figure 1. Biosynthesis and uses of malonyl-CoA analogues. Natural and engineered biosynthetic pathways for mCoA (**1**) and derivatives involve acyl-CoA ligases, acetyl-CoA dehydrogenases (AcDH), enoyl-CoA-reductases (ECR), malonyl-CoA synthetases, and various acyl-CoA carboxylases (propionyl-CoA carboxylase, PCC; acetyl-CoA carboxylase, ACC). Cosubstrates and cofactors are omitted for clarity. Examples of clinically relevant compounds that utilize malonyl-CoA and its derivatives are shown.

either an activator or a repressor in the presence of its native ligand, mCoA.[17]

Given its utility as a transcriptional regulator, FapR has been developed and utilized as a mCoA biosensor in several hosts, including *Escherichia coli*,[17−19] yeast,[20,21] and mammalian cells.[22] The first reported FapR biosensor in *E. coli* utilized the *fapR* gene from *Bacillus subtilis* cloned under T7 and LacI control alongside an *eGFP* reporter gene regulated by T7, LacI, and FapR (Figure 2A).[18] This FapR biosensor, while not initially optimized for a high signal-to-noise ratio, crucially established that a FapR biosensor could be used to quantify mCoA over a linear range suitable for most *in vivo* applications. The next iterations of the FapR biosensor in *E. coli* utilized a T7 promoter (FapR as a repressor) and a pGAP promoter

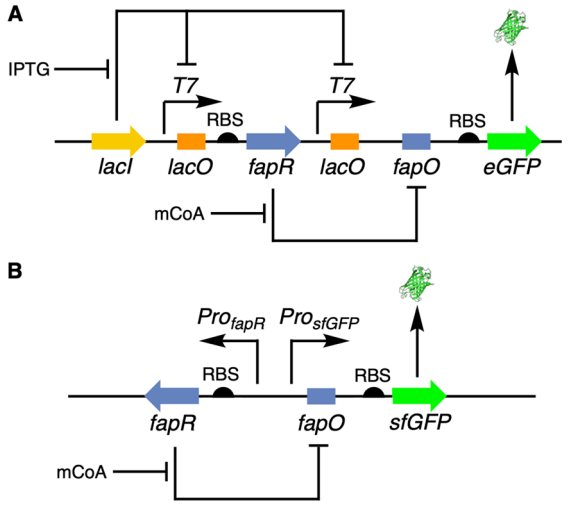

Figure 2. Redesigned malonyl-CoA biosensor. (A) Scheme showing a previous synthetic gene circuit regulated by IPTG and mCoA.[18] (B) Scheme showing a redesigned synthetic gene circuit regulated only by mCoA. At low levels of mCoA, FapR binds to its cognate operator and represses transcription. At increased levels, mCoA binds to FapR and causes a conformational change, allowing transcription of a fluorescent reporter gene. IPTG, isopropyl *β*-D-1-thiogalactopyranoside; *lacI*, *E. coli* lactose repressor; T7, bacteriophage T7 promoter; *lacO*, lacI repressor binding site; RBS, ribosome binding site; *fapR*, *B. subtilis* fatty acid biosynthetic pathway repressor; *fapO*, FapR repressor binding site; eGFP, enhanced GFP; mCoA, malonyl-CoA; $Pro_{fapR/sfGFP}$, constituitive *lac* promoters; *sfGFP*, superfolder GFP.

(FapR as an activator) to balance fatty acid biosynthesis against mCoA biosynthesis.[17] These biosensors were subsequently built with varying numbers of *fapO* sites placed downstream of the reporter gene promoter with the most sensitive of these unsurprisingly containing only a single operator sequence. FapR and LacI were also leveraged to create a fatty acid production negative feedback loop to alleviate the toxicity from acetyl-CoA carboxylase (*acc*) overexpression, leading to a one-third improvement in fatty acid titer in *E. coli*.[19] Notably, none of the previously reported FapR-based mCoA biosensors were utilized for detection of ligands beyond mCoA. Subsequently, they have been leveraged only for control of fatty acid products. Indeed, compounds related to mCoA such as acetyl-CoA, propionyl-CoA, succinyl-CoA, and butyryl-CoA have been reported to be noneffectors of FapR.[15] Furthermore, despite the important role of mCoA derivatives substituted at the C2 position as extender unit building blocks for many biologically relevant polyketides (Figure 1),[12,23−25] genetically encoded biosensors for C2-derivatives of mCoA have yet to be reported. Biosensors for such *α*-carboxyacyl-CoAs could be leveraged to optimize natural or artificial pathways that synthesize them in heterologous hosts.[26] Such sensors could also be used to dynamically regulate metabolic pathways that supply or consume natural or non-natural mCoA derivatives and lead to improvements in product titers of polyketide-derived metabolites that are dependent on natural or non-natural extender units.

Herein, we describe a FapR biosensor that requires no exogenous effectors (e.g., IPTG) and is optimized for a range of mCoA concentrations across a panel of *E. coli* strains. We also describe the development of a powerful cell-free transcription−translation (TX−TL) assay to probe the effector specificity of FapR toward a variety of non-native and non-natural acyl-thioesters. This enabled, for the first time, the discovery that the redesigned and optimized FapR-based biosensor detects several mCoA derivatives modified at the C2-position, providing a platform for the evaluation and evolution of the pathways necessary for their biosynthesis. Finally, we demonstrated the ability of the biosensor to detect the non-native polyketide extender unit methylmalonyl-CoA (mmCoA) produced in *E. coli*. In addition to detection and monitoring acyl-CoAs for chemical biology applications, biosensors with broad effector specificities also offer new

DOI: 10.1021/acssynbio.9b00078
ACS Synth. Biol. XXXX, XXX, XXX−XXX

Figure 3. Activation ratios of 93 variants from the FapR RBS library in *E. coli* 10G. The relative fluorescence (normalized to cell density) of each variant was determined at 0 and 25 μM cerulenin and divided to determine the fold activation. These values were compared with replicates (n = 3) of the prototype biosensor RBS (1A1, red).

Table 1. Biosensor Parameters in Various *E. coli* Strains

biosensor	RBS sequence[a]	TIR (au)[b]	*E. coli* strain	GFP_{min}[c]	GFP_{max}[d]	[cerulenin] (μM)[e]	$K_{1/2}$ (μM)[f]	activation ratio[g]
1A1	CAAGGAGGT	7594	DH5a	236 ± 2	18 000 ± 900	75	33.4 ± 0.5	77 ± 4
2H8	TACACAGGC	171	DH5a	1442 ± 44	50 000 ± 700	75	33.5 ± 1.1	34 ± 1
2H8	TACACAGGC	171	10G	2031 ± 127	58 000 ± 3000	50	20.3 ± 0.4	29 ± 2
2H8	TACACAGGC	171	TOP10	2203 ± 72	56 000 ± 2500	30	18.6 ± 1.0	25 ± 1

[a]Mutated nucleotides are underlined. [b]Transcription initiation rate (arbitrary units). [c]Relative GFP fluorescence at 0 mM cerulenin. [d]Highest measured relative GFP fluorescence. [e]Concentration of cerulenin that produced the highest measured relative GFP fluorescence. [f]Concentration of cerulenin at half-maximum relative GFP fluorescence, determined by fitting to the dose−response curve. [g]GFP_{max}/GFP_{min}

opportunities to overcome limitations of pathways that construct diverse α-carboxyacyl-CoAs and those pathways that depend on them.

RESULTS AND DISCUSSION

Refactoring the FapR Operon for an Efficient Prototype Malonyl-CoA Biosensor. Previously published *E. coli* malonyl-CoA biosensors were based on FapR as a repressor (with the addition of a second effector molecule, e.g. IPTG) or FapR as an activator.[17−19] Thus, these biosensors have been limited in their ability to be coupled with other protein expression systems and unnecessarily increase the metabolic burden on the host strain. To address this constraint, a biosensor construct was desired that required no external inputs to function and that was robust enough to use as a template for directed evolution of FapR or other proteins of interest. Toward this end, a new plasmid, pSENSE2FF, was designed based on our previously described macrolide biosensor.[4] Two constitutive *lac* promoters, Pro_{sfGFP} and Pro_{fapR} (pLacIQ),[4,27] control the transcription of a fluorescent reporter gene (superfolder GFP, *sfGFP*) and a codon-optimized version of the *fapR* gene from *B. subtilis*, respectively. Downstream of Pro_{sfGFP}, a single copy of the 17 bp *fapO* operator was introduced to afford FapR control of reporter transcription (Figure 2B and Supplementary Table S1). Superfolder GFP (sfGFP) was selected due to its higher brightness, rapid folding, and low photobleaching compared with other GFP variants.[28]

***In Vivo* Optimization of the Prototype Malonyl-CoA Biosensor.** Following the construction of the prototype refactored biosensor system, an *in vivo* assay utilizing cerulenin was developed to determine its fold activation. Because mCoA is not cell-permeable, it is not possible to directly manipulate its intracellular concentration. Cerulenin acts as an equimolar inhibitor of the β-keto-acyl-ACP synthase and causes a buildup of intracellular mCoA due to its inability to be processed to fatty acids,[29] although other impacts cannot be ruled out on the basis of its antibiotic activity.[30] The linear response of [mCoA] to [cerulenin] has been previously established for the concentrations used here.[18] The fold activation of the prototype biosensor strain (RBS 1A1) in response to mCoA was determined by measuring sfGFP fluorescence in the presence and absence of cerulenin supplemented to the culture media, revealing a modest activation ratio (approximately fivefold, Figure 3). Thus, the prototype biosensor required further optimization to enhance its sensitivity and fold-activation. It was hypothesized that lower concentrations of FapR would result in higher fluorescence output at a fixed concentration of mCoA, given that this could lead to less FapR bound to its cognate operator.[31−33] Therefore, the RBS of *fapR* was targeted for mutagenesis by designing an 18-member RBS variant library with a maximum calculated transcription initiation rate (TIR) equal to that of the RBS of 1A1 (7594 au). The fold-activation of ∼300 members of the *fapR* RBS library was determined by again leveraging cerulenin to enhance the intracellular concentration of mCoA (Figure 3). As predicted, most RBS variants resulted in significantly higher activation than the prototype 1A1 construct, with some reaching >60-fold activation under the assay conditions (Figure 3).

Several variants were selected from the FapR RBS library, and their dose−response curves with cerulenin were

DOI: 10.1021/acssynbio.9b00078
ACS Synth. Biol. XXXX, XXX, XXX−XXX

determined in *E. coli* DH5α (data not shown), a strain that showed the least toxicity toward the wide range of cerulenin concentrations used in preliminary screening (data not shown). One notable variant, 2H8, predicted to have the weakest calculated RBS (TIR = 171 au), provided a fluorescence output higher than that of 1A1 across the entire range of cerulenin concentrations assayed. The variant 2H8 also displayed a robust activation ratio (~34, Table 1) and provided a maximal fluorescent response of 58 000 RFU (relative fluorescence units) that was more than 3-fold higher than that of 1A1 (Figure 4 and Table 1). Notably, this

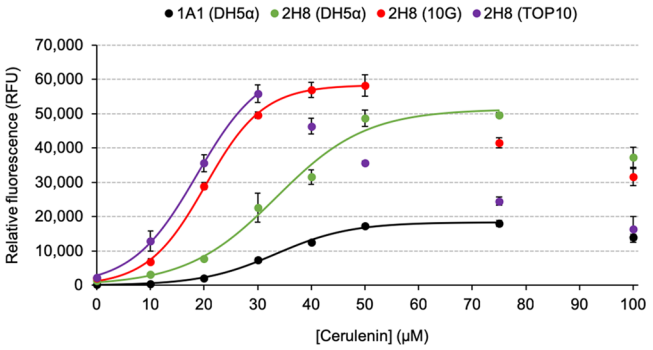

Figure 4. Cerulenin dose−response curves of the FapR biosensor in various *E. coli* strains. The relative fluorescence (normalized to cell density) was determined at each indicated cerulenin concentration, and the curves were fit to the Hill equation. Error bars (where visible) are the standard deviation of the mean (three biological replicates).

advantage came with the side effect of a leaky OFF state of ~1400 RFU, ~6-fold higher than that of 1A1, such that the $K_{1/2}$ of 2H8 with cerulenin was indistinguishable from that of 1A1 in this strain (Table 1). Nevertheless, this RBS engineering approach quickly arrived at a variant biosensor with the desired improvement in detection ability across a range of cerulenin concentrations.

FapR-Based Detection of Malonyl-CoA across Various *E. coli* Strains. The FapR-based biosensor inherently accounts for basal levels of ligand as mCoA is required for cell growth and is always present. However, the contribution of background mCoA to overall biosensor activity under other conditions cannot be easily subtracted because the levels of mCoA fluctuate significantly during growth of a culture.[17] Moreover, the effect of the inhibitor cerulenin across various strains of *E. coli* might not be consistent. To determine whether the engineered FapR biosensor response is dependent on the host strain, the best performing variant 2H8 was also transformed into *E. coli* 10G and *E. coli* TOP10, and the cerulenin dose−response curves were determined. Notably, there are differences in how the three *E. coli* strains respond to cerulenin, and consequently, the dose−response curves for each strain are significantly different (Figure 4 and Table 1). For example, the maximum fluorescence output of the FapR biosensor in *E. coli* TOP10, 10G, and DH5α is reached at ~30, ~50, and ~75 μM cerulenin, respectively (Table 1). In addition, the fluorescence output of the FapR biosensor in *E. coli* TOP10 at high concentrations of cerulenin (>50 μM) is significantly lower than that in *E. coli* DH5α or 10G (Figure 4). Thus, the FapR biosensor performs differently across various *E. coli* strains during growth of the culture but crucially always outperforms the prototype 1A1 in *E. coli* DH5α (Figure 4). The strain-specific dose−response curves might be a consequence of several factors, including unique FapR expression levels, unique sensitivity to cerulenin, or strain-dependent levels of mCoA in each strain. However, given that too much mCoA is toxic to the cell,[34,35] a culture with higher endogenous levels of mCoA is expected to result in both improved sensitivity to cerulenin and a lower fluorescence at lower concentrations of cerulenin. Interestingly, the few genomic differences between these strains are likely insufficient to directly explain large differences in mCoA production levels (Supplementary Table S2). Regardless, the overall robust performance of the FapR 2H8 biosensor across several strains of *E. coli* indicates that the engineered prototype biosensor is a good starting point for development of a tool for detection of other malonyl-CoA derivatives.

Probing the Effector Promiscuity of FapR by Cell-Free Transcription−Translation. Analysis of the crystal structure of FapR reveals that the terminal carboxylate of mCoA is a major factor in effector-binding specificity, forming a salt-bridge with the side chain of Arg106, and is facilitated by a nearby Phe99 side chain and Glu73′ backbone carbonyl (Figure 5A). In addition, the thioester of mCoA binds to the side chain of Asn115′.[15] Notably, while the side chain of Phe99 orients almost directly toward the α-carbon of mCoA (distance between Phe99-C_4 and mCoA-C_α is ~3.2 Å), there is room for substituents in place of the α-hydrogens of mCoA (especially in place of the *pro*-R hydrogen). Moreover, the loops that form the majority of the ligand binding pocket are disordered in the ligand-free FapR structure, which indicates this region is highly dynamic.[15] The lack of residues to restrict potential mCoA α-substituents coupled with the conformational flexibility suggest that mCoA derivatives might be FapR effectors. Accordingly, a series of mCoA derivatives with various alkyl and alkynyl functionalities at the C2-position was designed to probe the effector promiscuity of FapR and included mmCoA, ethylmalonyl-CoA (emCoA), propargylmalonyl-CoA (pgmCoA), and butylmalonyl-CoA (bmCoA) (Figure 5B). Furthermore, the 3′-phospho-nucleoside moiety of mCoA is solvent exposed (Figure 5A), suggesting that a large portion of CoA is not required for derepression of FapR. Accordingly, the truncated analogue mmSNAC was synthesized to test this hypothesis (Figure 5B).

Assessing the effector promiscuity of FapR *in vivo* with the panel of mCoA analogues is challenging for several reasons. First, acyl-CoAs are not cell-permeable and cannot be introduced exogenously. Second, pathways for assembling most non-native mCoA derivatives in *E. coli* have yet to be developed, limiting the high-level *in situ* biosynthesis of the selected acyl-CoAs. To circumvent these issues, a cell-free transcription−translation (TX−TL) approach was developed that could accurately control the concentration of mCoA within the assay.[36,37]

To this end, the reporter module of the FapR 2H8 biosensor was cloned into pET28a, replacing the typical *lacO* site controlling the T7 promoter with a single *fapO* binding site upstream of the *sfGFP* gene, producing pET28a-T7-fapO-sfGFP (Figure 5C). Each α-carboxyacyl-CoA was generated enzymatically from the corresponding malonic acid and CoA using the wild-type malonyl-CoA synthetase MatB or the engineered MatB variant, T207G/M306I.[38,39] Next, the response of the cell-free TX−TL biosensor assay was evaluated by using various concentrations of MatB-generated native effector, mCoA, along with a fixed amount of purified FapR and T7-fapO-sfGFP. The fluorescence output of the cell-free

DOI: 10.1021/acssynbio.9b00078
ACS Synth. Biol. XXXX, XXX, XXX−XXX

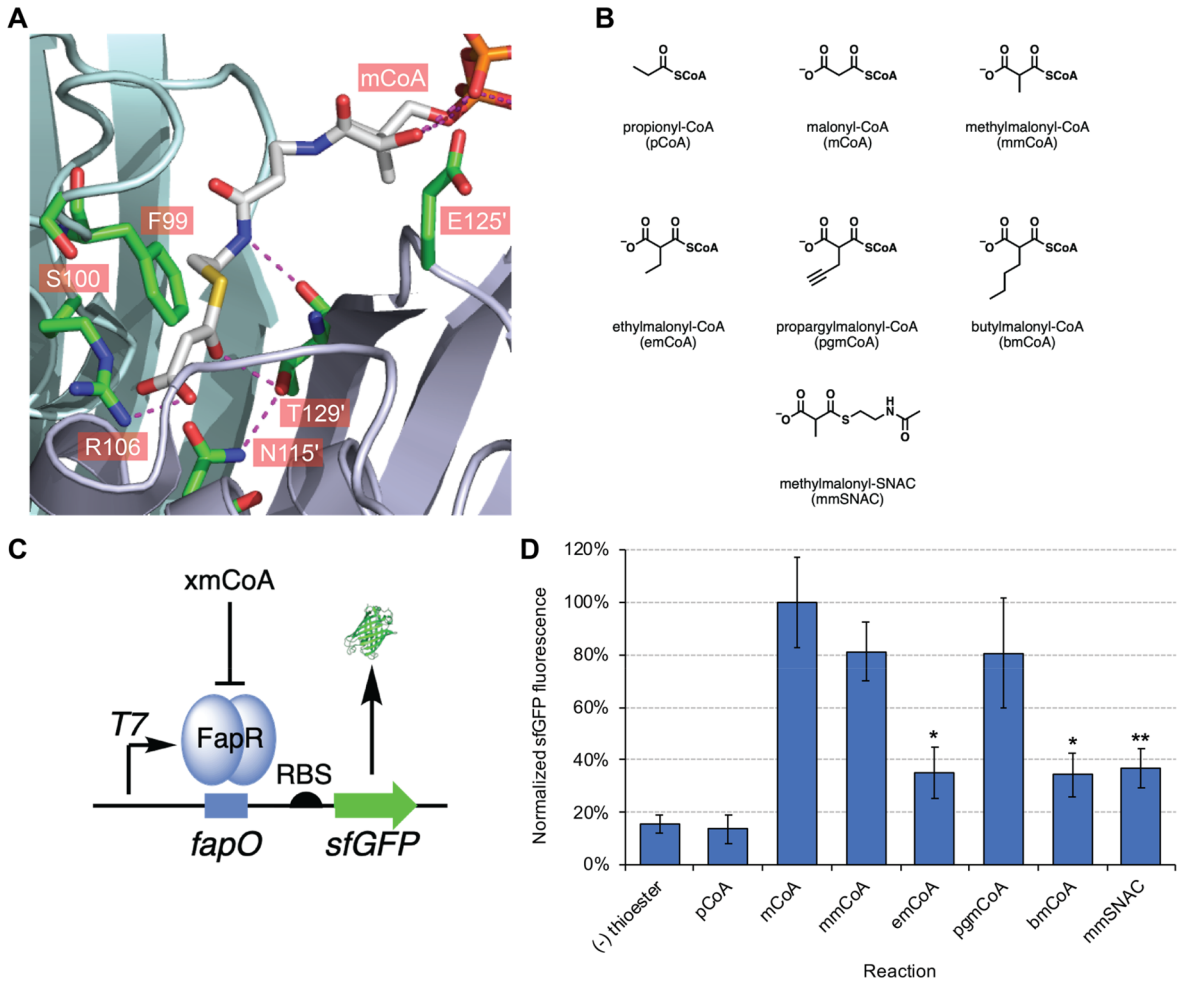

Figure 5. Probing the effector promiscuity of FapR with malonyl-CoA derivatives by cell-free transcription−translation. (A) The mCoA-binding pocket of FapR (PDB: 2F3X) with key residues highlighted (green sticks). Dashed lines are hydrogen bonds (purple). The bound mCoA is shown (white sticks). The ribbon structure of each subunit of the homodimer is shown in light green and light cyan. (B) Structures of each analogue tested with FapR. (C) Scheme showing the layout of the cell-free biosensor, pET28a-T7-fapO-sfGFP. (D) Fluorescence output of the cell-free biosensor pET28a-FapR/T7-fapO-sfGFP in the presence of each thioester at 200 μM. The output in the presence of the native effector mCoA is set to 100%. The (−) thioester control is boiled MatB. Error bars are the standard deviation of the mean (three biological replicates). *$p < 0.05$ by Student's unpaired two-tailed t test vs (−) thioester control. **$p < 0.01$ by Student's unpaired two-tailed t test vs (−) thioester control.

biosensor was approximately linear up to 150 μM mCoA (Supplementary Figure S1) and is consistent with previously reported *in vitro* transcription activities and binding affinities of FapR and mCoA.[40] In addition, the maximum fluorescence signal was ∼15-fold greater than that in the absence of mCoA. Furthermore, to account for potential inhibition of the cell-free biosensor by the MatB reaction mixture, the FapR system was also assayed using a commercial standard of mCoA. Notably, there was no significant difference in the fluorescence output of the cell-free FapR biosensor measured in the presence of the MatB-generated or commercial mCoA (Supplementary Figure S1). Together, these data indicate that the cell-free TX−TL assay is suitable to probe the effector promiscuity of FapR with MatB-generated xmCoAs.

Next, the cell-free FapR biosensor was assayed with each α-carboxyacyl-CoA at a fixed concentration (150 μM). Notably, the fluorescence response with mmCoA was statistically indistinguishable from that with the native ligand, mCoA (Figure 5D). Furthermore, the ethyl (emCoA), propargyl (pgmCoA), and butyl (bmCoA) derivatives of mCoA were all also identified as effectors, as judged by the cell-free fluorescence data. The ability of pgmCoA to derepress FapR/T7-fapO-sfGFP was indistinguishable from that of mCoA and mmCoA under the assay conditions used. The saturated alkyl derivatives emCoA and bmCoA were the poorest effectors based on the fluorescence data. This robust activity of pgmCoA may be due in part to the increased rigidity of the alkyne side chain or additional interactions of the alkynyl π-electrons with the FapR ligand-binding site, perhaps with the π-rich side chain of the nearby Phe99 (Figure 5A). Gratifyingly, as previously reported,[15] derepression was not observed in the presence of propionyl-CoA and was indistinguishable from the (−) thioester control. To provide further evidence that FapR is derepressed by derivatives of mCoA, FapR was tested *in vitro* for DNA-binding and release by electrophoretic mobility shift assay (EMSA) in the presence of mCoA or mmCoA. Using purified wild-type FapR protein, EMSA was run with a 40 bp DNA fragment containing the *fapO* binding site (Supplementary Figure S2). Incubation of the DNA fragment with a 2-fold excess of FapR resulted in near-complete binding and a corresponding gel shift. Next, to determine the concentration of mCoA at which half of the

DOI: 10.1021/acssynbio.9b00078
ACS Synth. Biol. XXXX, XXX, XXX−XXX

DNA would be bound, various concentrations of mCoA were titrated against FapR, revealing that 200 μM was required for this (data not shown). Incubation with the FapR-*fapO* complex with mmCoA achieved a similar level of derepression as that observed with mCoA (Supplementary Figure S2). Together, the *in vitro* data confirm the ability of mmCoA to derepress the FapR system.

In addition to the full-length α-carboxyacyl-CoAs, the truncated analogue mmSNAC was determined to be an effector, although it provided ~50% the derepression activity of the corresponding CoA thioester based upon the fluorescence assay (Figure 5D). Thus, even though a large portion of CoA is solvent exposed, some of the amide portion of CoA is still required for optimal derepression of FapR. Remarkably, and consistent with our structure-driven hypothesis, these data indicate that the promiscuity of FapR extends beyond the previously established native effector mCoA and includes non-native and non-natural malonyl-thioesters.

FapR-Based Detection of Methylmalonyl-CoA *in Vivo*. The discovery that FapR is derepressed by several non-native malonyl-CoA derivatives *in vitro* prompted us to consider whether the effector promiscuity of FapR could be leveraged to detect non-native acyl-CoAs inside living cells. As an initial test for FapR detection of derivatives of mCoA *in vivo*, a previously established and engineered *E. coli* strain optimized for high-level production of mmCoA was selected for analysis.[23] *E. coli* K207-3 includes the propionyl-CoA carboxylase (PCC) genes *pccB* and *accA1* from *Steptomyces coelicolor* under T7 polymerase/LacI control, allowing for production of mmCoA from propionate when induced with IPTG while endogenous mCoA levels remain unchanged.[41] Accordingly, the FapR biosensor 2H8 was introduced into the K207-3 strain, and the fluorescence output was determined in the presence or absence of IPTG/sodium propionate supplemented to the growth media. As expected, in the absence of IPTG, the fluorescence output was low (~2000 RFU) and similar to the background fluorescence of 2H8 in *E. coli* TOP10, 10G, and DH5α in the absence of cerulenin (Figure 6). Upon induction of the PCC genes with IPTG, the fluorescence output increased significantly (>15 000 RFU), even in the absence of supplemental propionate (Figure 6). Furthermore, a small and statistically significant increase in fluorescence signal was observed when the culture media was supplemented with sodium propionate. This indicates that in the absence of enzymatic machinery to otherwise consume mmCoA, and as previously reported,[24] there is sufficient endogenous propionate and/or propionyl-CoA in K207-3 to drive mmCoA biosynthesis to levels detectable by the engineered FapR biosensor.

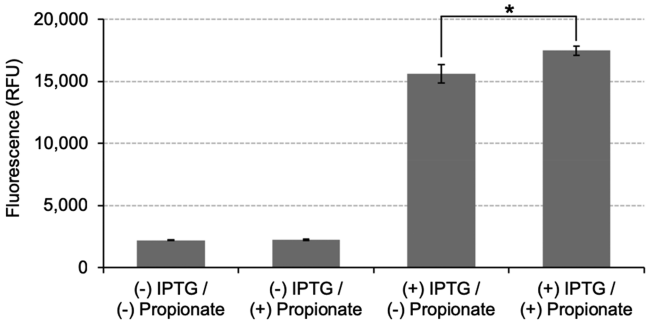

Figure 6. Detection of mmCoA in *E. coli* K207-3 by FapR 2H8. Fluorescence output of the 2H8 biosensor was determined in the absence/presence of 1 mM IPTG/1 mM propionate supplemented to the growth media. Error bars represent the standard deviation of three independent biological replicates. *p < 0.05 by Student's unpaired two-tailed t test.

DISCUSSION

The FapR transcription factor has been used extensively to monitor its native effector, mCoA,[21,22] and to regulate artificial genetic circuits that produce or consume mCoA.[17,19,20] Notably though, applications of FapR-based biosensors have been strictly limited due to their assumed strict specificity for mCoA. To address this deficiency, we set out to first optimize the FapR biosensor by simplifying its circuit architecture and leveraging RBS mutagenesis to improve its ability to detect mCoA in *E. coli*. By testing the engineered biosensor across a series of *E. coli* strains, the impact of different cellular backgrounds was highlighted, revealing that some aspects of the FapR-based detection of mCoA are host-dependent. Next, we probed the effector specificity of FapR beyond mCoA and prepared a panel of various α-carboxylmalonyl-thioesters via enzymatic or chemical synthesis. Crucially, a cell-free approach was developed to determine effector promiscuity with ligands that are otherwise cell impermeable. Moreover, the cell-free assay allowed the concentrations of each effector to be precisely controlled in the absence of other processes that might otherwise lead to fluctuations in their concentration over time. In this way, four additional CoA-thioesters were identified as effectors of FapR, including mmCoA, a metabolite native to *B. subtilis*. The biosensor was also shown to be derepressed by an α-carboxylmalonyl-SNAC, indicating that FapR could be harnessed to monitor intracellular levels of these chemically synthesized precursors that are frequently used as non-native and non-natural building blocks for polyketide biosynthesis. Remarkably, the native effector promiscuity of FapR was leveraged to detect mmCoA production in an engineered strain of *E. coli*, K207-3. It is notable that even though the abilities of mCoA and mmCoA to derepress FapR are indistinguishable (Figure 5D), the endogenous mCoA levels in K207-3 are not impacted by IPTG induction and/or propionate addition so that the expected increase in mmCoA production upon induction is easily detected by the FapR biosensor in K207-3. This result demonstrates the ability of the FapR biosensor to detect fluctuations in mmCoA in engineered microbial strains and paves the way to utilize this ability to guide improvements in mmCoA production and develop strategies for dynamic metabolic control of mmCoA-dependent pathways. It is possible that further engineering of the FapR effector binding pocket would enable the detection of additional ligands or even specificity toward individual ligands, especially given the precedent of manipulating the effector specificity of other transcription-factor-based biosensors.[4,42]

This work has identified FapR as a tool for regulating metabolic pathways that produce or consume mmCoA. Moreover, the ability of FapR to detect various α-carboxylmalonyl-CoAs now sets the stage for high-throughput engineering approaches such as directed evolution to be applied to enzymatic pathways responsible for the biosynthesis of natural or non-natural malonyl-CoA derivatives in diverse microbial hosts.[26,43,44] In this way, we anticipate that FapR will prove an invaluable device to expand the scope and utility of a broad range of microbial-based platforms for synthesis of products constructed from diverse polyketide extender units.

DOI: 10.1021/acssynbio.9b00078
ACS Synth. Biol. XXXX, XXX, XXX−XXX

MATERIALS AND METHODS

General. Materials and reagents were purchased from Sigma-Aldrich (St. Louis, MO) unless otherwise noted. Isopropyl β-D-thiogalactoside (IPTG) was purchased from Calbiochem (Gibbstown, NJ). Primers were purchased from Integrated DNA Technologies (Coralville, IA). *E. cloni* 10G electrocompetent cells were purchased from Lucigen Corporation (Middleton, WI). Cerulenin was purchased from Cayman Chemical (Ann Arbor, MI), and stocks were dissolved in DMSO. Commercial malonyl-CoA and methylmalonyl-CoA were purchased from CoALA Biosciences (Austin, TX). All cultures were grown in LB media with 100 μg/mL ampicillin unless otherwise stated. Absorbance and fluorescence readings were taken in clear flat-bottom and black flat-bottom 96-well plates (Greiner Bio-One), respectively, in a BioTek Hybrid Synergy 4 plate reader unless otherwise stated. All Sanger sequencing was performed by Genewiz, Inc. (South Plainfield, NJ).

Construction of Plasmids. The plasmid pSENSE2 was synthesized by Twist Bioscience (San Francisco, CA) in two fragments. The two pieces were assembled using standard restriction digestion and ligation procedures. The fapR_fapO fragment containing a codon-optimized *fapR* gene and a *fapO* operator was synthesized by Genewiz, Inc. and cloned into pSENSE2 between the *Kpn*I and *Spe*I sites to give pSENSE2FF. *FapR* was amplified with a 5′ *Nco*I site and a 3′ *Xho*I site and cloned into pET28a to give fapR_pET28a (with a C-terminal His_6 tag). T7_fapO_sfGFP was constructed using GenScript GenBuilder (GenScript, Piscataway, NJ) according to the manufacturer's instructions with pET28a (amplified with T7forfapO.Gib1 and T7forfapO.Gib2, see entries 1 and 2, Supplementary Table S3) and fapO_sfGFP (amplified from pSENSE2FF with fapOforT7.Gib1 and fapOforT7.Gib2, see entries 3 and 4, Supplementary Table S3).

RBS Library Construction and Screening. The original *fapR* RBS 1A1 was calculated to have a transcription initiation rate (TIR) of 7594 au using the Salis online RBS calculator.[31−33] The calculator was used to design an 18-member RBS library with a maximum TIR of 7594 au. Site-directed mutagenesis was also used to produce the RBS library (VRGAGGH) using the QuikChange II Site-Directed Mutagenesis protocol with the pSENSE2FF template and primers FapR_RBSLib2.SDM1 and FapR_RBSLib2.SDM2 (see entries 5 and 6, Supplementary Table S3). The reaction product was digested with *Dpn*I for 3 h at 37 °C before electroporation into *E. cloni* 10G electrocompetent cells (Lucigen). Transformed cells were plated on LB agar supplemented with 100 μg/mL ampicillin and incubated overnight at 37 °C. Individual colonies from the library were picked from LB agar plates and used to inoculate 93 wells of a 96-deepwell microplate with 500 μL of LB media supplemented with 100 μg/mL ampicillin. The remaining three wells were inoculated with colonies from pSENSE2FF RBS 1A1 that had been transformed into *E. coli* DH5α. Cultures were grown overnight at 37 °C and 350 rpm, and 10 μL from each well were used to inoculate 440 μL LB media supplemented with 100 μg/mL ampicillin. The new plates were grown for 1 h at 37 °C and 350 rpm. Plates were then treated with either 5, 12.5, or 25 μM cerulenin or the corresponding volume of DMSO. Plates were then grown an additional 15 h. Plates were centrifuged at 3500 rpm for 7 min, and cell pellets were resuspended in 500 μL of PBS. One hundred microliters from each well was used for analyzing optical density at 600 nm and sfGFP fluorescence (ex 485 nm/em 509 nm). Fluorescence values were divided by OD_{600} to yield growth-corrected relative fluorescence values. Two hundred and seventy-nine individual colonies from the RBS library were screened at the different cerulenin concentrations.

Expression and Purification of Mutant MatB. The expression and purification of MatB T207G/M306I has been previously described.[38,39,45] Briefly, *E. coli* BL21(DE3) pLysS competent cells were transformed with plasmid, and positive transformants were selected on LB agar supplemented with 30 μg/mL kanamycin. A single colony was transferred to LB (3 mL) supplemented with kanamycin (30 μg/mL) and grown at 37 °C and 250 rpm overnight. The culture was used to inoculate LB media (1 L) supplemented with kanamycin (30 μg/mL). One liter of culture was incubated at 37 °C and 250 rpm to an OD_{600} of 0.6, at which time protein synthesis was induced by the addition of IPTG to a final concentration of 1 mM. After incubation at 18 °C and 200 rpm for 18 h, cells were collected by centrifugation at 5000*g* for 20 min, resuspended in 100 mM Tris-HCl pH 8.0 (20 mL) containing NaCl (300 mM), and then lysed by sonication. Following centrifugation at 10 000*g*, the soluble extract was loaded onto a 1 mL HisTrap HP column (GE Healthcare, Piscataway, NJ) and purified by fast protein liquid chromatography using the following buffers: wash buffer [20 mM sodium phosphate (pH 7.4) containing 0.5 M NaCl and 20 mM imidazole] and elution buffer [20 mM sodium phosphate (pH 7.4) containing 0.5 M NaCl and 200 mM imidazole]. The purified protein was concentrated using an Amicon Ultra 30 kDa MWCO centrifugal filter (Millipore Corp., Billerica, MA) and stored as 10% glycerol stocks at −80 °C. Protein purity was verified by SDS-PAGE. Protein quantification was carried out using the Bradford Protein Assay Kit from Bio-Rad.

Synthesis of Acyl-CoAs by MatB. The MatB-catalyzed synthesis of extender units has been previously described.[38,39,45] Briefly, reactions were performed in a 50 μL reaction mixture containing 100 mM sodium phosphate (pH 7), $MgCl_2$ (2 mM), ATP (12 mM), coenzyme A (8 mM), malonate or corresponding analogue (16 mM), and wild-type or mutant MatB (10 μg) at 25 °C. Aliquots were removed after 3 h of incubation and quenched with an equal volume of ice-cold methanol and centrifuged at 10 000*g* for 10 min, and cleared supernatants were used for HPLC analysis on a Varian ProStar HPLC system. A series of linear gradients was developed from 0.1% TFA (A) in water to methanol (HPLC grade, B) using the following protocol: 0−32 min, 80% B; 32−35 min, 100% A. The flow rate was 1 mL/min, and the absorbance was monitored at 254 nm using Pursuit XRs C18 column (250 × 4.6 mm, Varian Inc.). To ensure complete conversion, the malonate analogue and the acyl-CoA product HPLC peak areas were integrated, and the conversion (%) was calculated as a percent of the total peak area. Product elution times and LC-MS data (data not shown) were in complete agreement with those previous described.[38,45]

Synthesis of mmSNAC. To access the previously reported mmSNAC, the α-carboxy group of the corresponding commercial methylmalonic acid was protected via esterification with ^{t}Bu, which was then thioesterified with HSNAC, and deprotected via hydrolysis to afford the acyl-SNAC.[46−48] Full synthetic methods and product characterization can be found in the Supplemental Methods.

DOI: 10.1021/acssynbio.9b00078
ACS Synth. Biol. XXXX, XXX, XXX−XXX

Cell-Free Characterization of FapR Promiscuity. A commercial kit for cell-free transcription−translation reactions was purchased from New England Biolabs (PURExpress In Vitro Protein Synthesis Kit). To a PCR tube on ice were added (in the order shown): 4 μL Solution A, 3 μL Solution B, 2.5 μM FapR, 250 nM T7-fapO-sfGFP, and 150 μM of MatB-generated acyl-CoA or mmSNAC in a total volume of 10 μL. In parallel, control reactions in the absence of thioester were assembled by using boiled MatB. The reaction was incubated for 16 h at 37 °C and then diluted with PBS buffer to give a final total volume of 50 μL. Then, the diluted mixture was used for determination of the sfGFP fluorescence (ex 485 nm/em 510 nm) using a Tecan infinite F200 microplate spectrophotometer.

FapR-Bioassay of Methylmalonyl-CoA Production in *E. coli* K207-3. pSENSE2FF-2H8 was transformed into *E. coli* K207-3 and grown overnight in 1 mL volumes in a 96-deepwell microplate at 37 °C and 350 rpm. These cultures (10 μL) were used to inoculate wells of a fresh 96-deepwell plate containing 440 μL LB and 100 μg mL^{-1} ampicillin which were then incubated at 37 °C and 350 rpm for 2.5 h. Various combinations of IPTG (1 mM final concentration) and sodium propionate (1 mM final concentration) were then added, and the cultures were incubated for 16 h at 37 °C and 350 rpm. The microplate was centrifuged at 3500 rpm for 7 min, and the supernatant was discarded. Cell pellets were resuspended in 1 mL PBS, and 100 μL of each cell suspension was transferred to flat-bottom 96-well plates and used for determining the optical density at 600 nm (OD_{600}) and sfGFP fluorescence (ex 485 nm/em 509 nm). The fluorescence intensity was divided by the OD_{600} to yield a relative GFP fluorescence value.

Purification of FapR. *E. coli* BL21(DE3) competent cells were transformed with fapR_pET28a plasmid, and positive transformants were selected on LB agar supplemented with 30 μg/mL kanamycin. A single colony was transferred to LB (3 mL) supplemented with kanamycin (30 μg/mL) and grown at 37 °C and 250 rpm overnight. The culture was used to inoculate LB media (300 mL) supplemented with kanamycin (30 μg/mL). The culture was incubated at 37 °C and 250 rpm to an OD_{600} of 0.6, at which time protein synthesis was induced by the addition of IPTG to a final concentration of 1 mM. After incubation at 22 °C and 250 rpm for 20 h, cells were collected by centrifugation at 5000*g* for 20 min, resuspended in 100 mM Tris-HCl pH 8.0 (8 mL) containing NaCl (300 mM), and then lysed by sonication. Following centrifugation at 10 000*g*, the soluble extract was loaded onto a 1 mL HisTrap HP column (GE Healthcare, Piscataway, NJ) and purified by fast protein liquid chromatography using the following buffers: wash buffer [20 mM sodium phosphate (pH 7.4) containing 0.5 M NaCl and 20 mM imidazole] and elution buffer [20 mM sodium phosphate (pH 7.4) containing 0.5 M NaCl and 200 mM imidazole]. The purified protein was concentrated using an Amicon Ultra 10 kDa MWCO centrifugal filter (Millipore Corp., Billerica, MA) and stored in storage buffer (50 mM HEPES, pH 7.5, 100 mM NaCl, and 10% glycerol) at −80 °C. Protein purity was verified by SDS-PAGE. Protein quantification was carried out using the Bradford Protein Assay Kit from Bio-Rad.

■ ASSOCIATED CONTENT

Supporting Information

The Supporting Information is available free of charge on the ACS Publications website at DOI: 10.1021/acssynbio.9b00078.

Includes supplementary tables, supplemental figures, and detailed methods that describe the synthesis of mmSNAC, dose−response of the cell-free TX−TL assay, and electrophoretic mobility shift assay (PDF)

■ AUTHOR INFORMATION

Corresponding Author

*E-mail: gjwillia@ncsu.edu.

ORCID

Edward Kalkreuter: 0000-0002-8241-4455

Gavin J. Williams: 0000-0003-2172-9063

Present Addresses

§E.K.: Department of Chemistry, The Scripps Research Institute, Jupiter, Florida 33458, United States.

⊥K.S.B.: UNC Chapel Hill School of Medicine, Chapel Hill, North Carolina 27516, United States.

Author Contributions

¶A.M.K. and A.A.M. contributed equally.

Notes

The authors declare no competing financial interest.

■ ACKNOWLEDGMENTS

This study was supported in part by National Institutes of Health grants GM104258 and GM124112 (G.J.W.).

■ REFERENCES

(1) Kasey, C., and Williams, G. J. (2018) Chapter 8: Customizing transcription-factor biosensors for modern biotechnology. In *Modern Biocatalysis: Advances Towards Synthetic Biological Systems*, pp 203−233, The Royal Society of Chemistry.

(2) Carpenter, A. C., Paulsen, I. T., and Williams, T. C. (2018) Blueprints for biosensors: design, limitations, and applications. *Genes 9*, 375.

(3) Shi, S., Ang, E. L., and Zhao, H. (2018) In vivo biosensors: mechanisms, development, and applications. *J. Ind. Microbiol. Biotechnol. 45*, 491−516.

(4) Kasey, C. M., Zerrad, M., Li, Y., Cropp, T. A., and Williams, G. J. (2018) Development of transcription factor-based designer macrolide biosensors for metabolic engineering and synthetic biology. *ACS Synth. Biol. 7*, 227−239.

(5) Zhang, F., Carothers, J. M., and Keasling, J. D. (2012) Design of a dynamic sensor-regulator system for production of chemicals and fuels derived from fatty acids. *Nat. Biotechnol. 30*, 354−359.

(6) Siedler, S., Schendzielorz, G., Binder, S., Eggeling, L., Bringer, S., and Bott, M. (2014) SoxR as a single-cell biosensor for NADPH-consuming enzymes in *Escherichia coli*. *ACS Synth. Biol. 3*, 41−47.

(7) Dahl, R. H., Zhang, F., Alonso-Gutierrez, J., Baidoo, E., Batth, T. S., Redding-Johanson, A. M., Petzold, C. J., Mukhopadhyay, A., Lee, T. S., Adams, P. D., and Keasling, J. D. (2013) Engineering dynamic pathway regulation using stress-response promoters. *Nat. Biotechnol. 31*, 1039−1046.

(8) Johnson, A. O., Gonzalez-Villanueva, M., Wong, L., Steinbuchel, A., Tee, K. L., Xu, P., and Wong, T. S. (2017) Design and application of genetically-encoded malonyl-CoA biosensors for metabolic engineering of microbial cell factories. *Metab. Eng. 44*, 253−264.

(9) Fowler, Z. L., Gikandi, W. W., and Koffas, M. A. (2009) Increased malonyl coenzyme A biosynthesis by tuning the *Escherichia coli* metabolic network and its application to flavanone production. *Appl. Environ. Microbiol. 75*, 5831−5839.

DOI: 10.1021/acssynbio.9b00078
ACS Synth. Biol. XXXX, XXX, XXX−XXX

(10) Leonard, E., Yan, Y., Fowler, Z. L., Li, Z., Lim, C. G., Lim, K. H., and Koffas, M. A. (2008) Strain improvement of recombinant *Escherichia coli* for efficient production of plant flavonoids. *Mol. Pharmaceutics 5*, 257−265.
(11) Walker, M. C., Thuronyi, B. W., Charkoudian, L. K., Lowry, B., Khosla, C., and Chang, M. C. (2013) Expanding the fluorine chemistry of living systems using engineered polyketide synthase pathways. *Science 341*, 1089−1094.
(12) Dayem, L. C., Carney, J. R., Santi, D. V., Pfeifer, B. A., Khosla, C., and Kealey, J. T. (2002) Metabolic engineering of a methylmalonyl-CoA mutase-epimerase pathway for complex polyketide biosynthesis in *Escherichia coli*. *Biochemistry 41*, 5193−5201.
(13) Lombo, F., Pfeifer, B., Leaf, T., Ou, S., Kim, Y. S., Cane, D. E., Licari, P., and Khosla, C. (2001) Enhancing the atom economy of polyketide biosynthetic processes through metabolic engineering. *Biotechnol. Prog. 17*, 612−617.
(14) Schujman, G. E., Paoletti, L., Grossman, A. D., and de Mendoza, D. (2003) FapR, a bacterial transcription factor involved in global regulation of membrane lipid biosynthesis. *Dev. Cell 4*, 663−672.
(15) Schujman, G. E., Guerin, M., Buschiazzo, A., Schaeffer, F., Llarrull, L. I., Reh, G., Vila, A. J., Alzari, P. M., and de Mendoza, D. (2006) Structural basis of lipid biosynthesis regulation in Gram-positive bacteria. *EMBO J. 25*, 4074−4083.
(16) Albanesi, D., Reh, G., Guerin, M. E., Schaeffer, F., Debarbouille, M., Buschiazzo, A., Schujman, G. E., de Mendoza, D., and Alzari, P. M. (2013) Structural basis for feed-forward transcriptional regulation of membrane lipid homeostasis in *Staphylococcus aureus*. *PLoS Pathog. 9*, No. e1003108.
(17) Xu, P., Li, L., Zhang, F., Stephanopoulos, G., and Koffas, M. (2014) Improving fatty acids production by engineering dynamic pathway regulation and metabolic control. *Proc. Natl. Acad. Sci. U. S. A. 111*, 11299−11304.
(18) Xu, P., Wang, W., Li, L., Bhan, N., Zhang, F., and Koffas, M. A. (2014) Design and kinetic analysis of a hybrid promoter-regulator system for malonyl-CoA sensing in *Escherichia coli*. *ACS Chem. Biol. 9*, 451−458.
(19) Liu, D., Xiao, Y., Evans, B. S., and Zhang, F. (2015) Negative feedback regulation of fatty acid production based on a malonyl-CoA sensor-actuator. *ACS Synth. Biol. 4*, 132−140.
(20) David, F., Nielsen, J., and Siewers, V. (2016) Flux control at the malonyl-CoA node through hierarchical dynamic pathway regulation in *Saccharomyces cerevisiae*. *ACS Synth. Biol. 5*, 224−233.
(21) Li, S., Si, T., Wang, M., and Zhao, H. (2015) Development of a synthetic malonyl-CoA sensor in *Saccharomyces cerevisiae* for intracellular metabolite monitoring and genetic screening. *ACS Synth. Biol. 4*, 1308−1315.
(22) Ellis, J. M., and Wolfgang, M. J. (2012) A genetically encoded metabolite sensor for malonyl-CoA. *Chem. Biol. 19*, 1333−1339.
(23) Murli, S., Kennedy, J., Dayem, L. C., Carney, J. R., and Kealey, J. T. (2003) Metabolic engineering of *Escherichia coli* for improved 6-deoxyerythronolide B production. *J. Ind. Microbiol. Biotechnol. 30*, 500−509.
(24) Zhang, H., Boghigian, B. A., and Pfeifer, B. A. (2010) Investigating the role of native propionyl-CoA and methylmalonyl-CoA metabolism on heterologous polyketide production in *Escherichia coli*. *Biotechnol. Bioeng. 105*, 567−573.
(25) Cai, W., and Zhang, W. (2018) Engineering modular polyketide synthases for production of biofuels and industrial chemicals. *Curr. Opin. Biotechnol. 50*, 32−38.
(26) Chan, Y. A., Podevels, A. M., Kevany, B. M., and Thomas, M. G. (2009) Biosynthesis of polyketide synthase extender units. *Nat. Prod. Rep. 26*, 90.
(27) Penumetcha, P., Lau, K., Zhu, X., Davis, K., Eckdahl, T. T., and Campbell, A. M. (2010) Improving the Lac system for synthetic biology. *Bios 81*, 7−15.
(28) Shaner, N. C., Lambert, G. G., Chammas, A., Ni, Y., Cranfill, P. J., Baird, M. A., Sell, B. R., Allen, J. R., Day, R. N., Israelsson, M., Davidson, M. W., and Wang, J. (2013) A bright monomeric green fluorescent protein derived from *Branchiostoma lanceolatum*. *Nat. Methods 10*, 407−409.
(29) Price, A. C., Choi, K. H., Heath, R. J., Li, Z., White, S. W., and Rock, C. O. (2001) Inhibition of beta-ketoacyl-acyl carrier protein synthases by thiolactomycin and cerulenin. Structure and mechanism. *J. Biol. Chem. 276*, 6551−6559.
(30) Goldberg, I., Walker, J. R., and Bloch, K. (1973) Inhibition of lipid synthesis in Escherichia coli cells by the antibiotic cerulenin. *Antimicrob. Agents Chemother. 3*, 549−554.
(31) Espah Borujeni, A., Channarasappa, A. S., and Salis, H. M. (2014) Translation rate is controlled by coupled trade-offs between site accessibility, selective RNA unfolding and sliding at upstream standby sites. *Nucleic Acids Res. 42*, 2646−2659.
(32) Salis, H. M., Mirsky, E. A., and Voigt, C. A. (2009) Automated design of synthetic ribosome binding sites to control protein expression. *Nat. Biotechnol. 27*, 946−950.
(33) Farasat, I., Kushwaha, M., Collens, J., Easterbrook, M., Guido, M., and Salis, H. M. (2014) Efficient search, mapping, and optimization of multi-protein genetic systems in diverse bacteria. *Mol. Syst. Biol. 10*, 731.
(34) Pizer, E. S., Thupari, J., Han, W. F., Pinn, M. L., Chrest, F. J., Frehywot, G. L., Townsend, C. A., and Kuhajda, F. P. (2000) Malonyl-coenzyme-A is a potential mediator of cytotoxicity induced by fatty-acid synthase inhibition in human breast cancer cells and xenografts. *Cancer Res. 60*, 213−218.
(35) Thupari, J. N., Pinn, M. L., and Kuhajda, F. P. (2001) Fatty acid synthase inhibition in human breast cancer cells leads to malonyl-CoA-induced inhibition of fatty acid oxidation and cytotoxicity. *Biochem. Biophys. Res. Commun. 285*, 217−223.
(36) Nagaraj, V. H., Greene, J. M., Sengupta, A. M., and Sontag, E. D. (2017) Translation inhibition and resource balance in the TX−TL cell-free gene expression system, *Synthetic Biology 2*. DOI: 10.1093/synbio/ysx005
(37) Wang, H., Jewett, M. C., and Li, J. (2018) Development of a *Pseudomonas putida* cell-free protein synthesis platform for rapid screening of gene regulatory elements, *Synthetic Biology 3*. DOI: 10.1093/synbio/ysy003
(38) Koryakina, I., McArthur, J., Randall, S., Draelos, M. M., Musiol, E. M., Muddiman, D. C., Weber, T., and Williams, G. J. (2013) Poly specific trans-acyltransferase machinery revealed via engineered acyl-CoA synthetases. *ACS Chem. Biol. 8*, 200−208.
(39) Koryakina, I., and Williams, G. J. (2011) Mutant malonyl-CoA synthetases with altered specificity for polyketide synthase extender unit generation. *ChemBioChem 12*, 2289−2293.
(40) Martinez, M. A., Zaballa, M. E., Schaeffer, F., Bellinzoni, M., Albanesi, D., Schujman, G. E., Vila, A. J., Alzari, P. M., and de Mendoza, D. (2010) A novel role of malonyl-ACP in lipid homeostasis. *Biochemistry 49*, 3161−3167.
(41) Rodriguez, E., and Gramajo, H. (1999) Genetic and biochemical characterization of the alpha and beta components of a propionyl-CoA carboxylase complex of *Streptomyces coelicolor* A3(2). *Microbiology 145*, 3109−3119.
(42) Taylor, N. D., Garruss, A. S., Moretti, R., Chan, S., Arbing, M. A., Cascio, D., Rogers, J. K., Isaacs, F. J., Kosuri, S., Baker, D., Fields, S., Church, G. M., and Raman, S. (2016) Engineering an allosteric transcription factor to respond to new ligands. *Nat. Methods 13*, 177−183.
(43) Vogeli, B., Geyer, K., Gerlinger, P. D., Benkstein, S., Cortina, N. S., and Erb, T. J. (2018) Combining promiscuous acyl-CoA oxidase and enoyl-CoA carboxylase/reductases for atypical polyketide extender unit biosynthesis. *Cell Chem. Biol. 25*, 833−839 e834.
(44) Peter, D. M., Vogeli, B., Cortina, N. S., and Erb, T. J. (2016) A chemo-enzymatic road map to the synthesis of CoA esters. *Molecules 21*, 517.
(45) Koryakina, I., McArthur, J. B., Draelos, M. M., and Williams, G. J. (2013) Promiscuity of a modular polyketide synthase towards natural and non-natural extender units. *Org. Biomol. Chem. 11*, 4449−4458.

DOI: 10.1021/acssynbio.9b00078
ACS Synth. Biol. XXXX, XXX, XXX−XXX

(46) Hansen, D. A., Rath, C. M., Eisman, E. B., Narayan, A. R., Kittendorf, J. D., Mortison, J. D., Yoon, Y. J., and Sherman, D. H. (2013) Biocatalytic synthesis of pikromycin, methymycin, neomethymycin, novamethymycin, and ketomethymycin. *J. Am. Chem. Soc. 135*, 11232−11238.
(47) Li, Y., Zhang, W., Zhang, H., Tian, W., Wu, L., Wang, S., Zheng, M., Zhang, J., Sun, C., Deng, Z., Sun, Y., Qu, X., and Zhou, J. (2018) Structural basis of a broadly selective acyltransferase from the polyketide synthase of splenocin. *Angew. Chem., Int. Ed. 57*, 5823−5827.
(48) Mo, S., Kim, D. H., Lee, J. H., Park, J. W., Basnet, D. B., Ban, Y. H., Yoo, Y. J., Chen, S. W., Park, S. R., Choi, E. A., Kim, E., Jin, Y. Y., Lee, S. K., Park, J. Y., Liu, Y., Lee, M. O., Lee, K. S., Kim, S. J., Kim, D., Park, B. C., Lee, S. G., Kwon, H. J., Suh, J. W., Moore, B. S., Lim, S. K., and Yoon, Y. J. (2011) Biosynthesis of the allylmalonyl-CoA extender unit for the FK506 polyketide synthase proceeds through a dedicated polyketide synthase and facilitates the mutasynthesis of analogues. *J. Am. Chem. Soc. 133*, 976−985.

DOI: 10.1021/acssynbio.9b00078
ACS Synth. Biol. XXXX, XXX, XXX−XXX